Effect of Tyrosine to Alanine Mutation on the Dimerization Process of -Synuclein: A Potential of Mean Force study

Airy Sanjeev and Venkata Satish Kumar Mattaparthi
Molecular Modelling and Simulation Laboratory,
Department of Molecular Biology and Biotechnology, Tezpur University, Tezpur-784 028, Assam, India

(Corresponding author: Venkata Satish Kumar Mattaparthi, mvenkatasatishkumar@gmail.com)

ABSTRACT: Aggregation of -synuclein into well-ordered amyloid fibrils is associated with the pathogenesis of Parkinson's disease. Several studies have suggested that Tyrosine residues of -synuclein are involved in the intra and inter-molecular interactions during the fibrillation process. Here we demonstrate the role of tyrosine residues on the inter-molecular interactions during fibrillation process by analyzing the effect of tyrosine to alanine mutation on dimerization process of -synuclein. We modeled the homo-dimer complex of the three tyrosine mutants: (Y39A; Y133A; Y (125,133,136)A) and Wild type -synuclein and carried out potential of mean force study to analyze and compare free energy profile. We observed the minimum of separation of monomeric units to be smaller in Y39A and larger in Y133A dimer. Therefore we see Y39A mutation to accelerate the aggregation while Y133A slow down the aggregation. So the methods targeting tyrosine residue at position 133 may be helpful to reduce the aggregation propensity.

Keywords: Aggregation, Parkinson's disease, mutants, free energy, fibrillation

INTRODUCTION

 -Synuclein belongs to the class of Intrinsically Disordered Proteins (Fauvet *et al.,* 2012; Iwai *et al.,* 1995; Weinreb *et al.,* 1996) consisting of 140 amino acids (Bisaglia *et al.,* 2009). The aggregation of -synuclein into well-ordered fibrils has been associated with the onset of Parkinson's disease and various other neurodegenerative diseases (Uversky *et al.,* 2009). However, the exact mechanism is still not known. Although the protein-lipid interaction involved in -synuclein appears to be an important factor for the physio-pathological characteristics of the protein (Bendor *et al*., 2013; Pirc *et al*., 2011). The fibrillation of -synuclein is a nucleation-dependent process which is associated with the transformation of unfolded monomer into oligomers and then to fibrils wherein the cross- -sheet are formed (Breydo *et al*., 2012; Fink 2006; Serpell *et al*., 2000; Uversky *et al*., 2001). However the increased hydrophobic exposure is associated with the transformed monomeric and oligomeric species (Cremades *et al*., 2012; Dusa *et al*., 2006; Uversky *et al*., 2001). -Synuclein protein consists of three structural components: N-terminal (1-60), which is highly conserved and positively charged;NAC (non-amyloid component) domain (61-95), the aggregation prone region (Giasson *et al*., 2001) and the C-terminal (96-140) which is acidic and negatively charged. The presence of aromatic residues present in -synuclein have been suggested to play a critical role in self-assembly and molecular recognition for the formation of amyloid (Gazit, 2002). There are four Tyr residues in the two terminals of -synuclein protein that are placed at positions 39,125,133 and 136. The presence of these residues plays an important factor in the aggregation propensity of -synuclein. Several intra-molecular contacts of -synuclein are crucial which involve the electrostatic and hydrophobic interactions (Bertoncini *et al*., 2005). Studies have suggested that fibrillation process can be inhibited by interruption of these hydrophobic intra-molecular interactions (Ulrih *et al*., 2008). It has also been recently suggested that Tyr residues of -synuclein also play important role in inter-molecular interactions during the fibrillation process (Izawa *et al*., 2012). Due to this, the modifications of Tyr residues through various *in vivo* studies have been known to affect the fibrillation propensity (Lamberto *et al*., 2009; Ulrih *et al*., 2008; Yamin *et al*., 2003).

In order to investigate the inter-molecular interactions involving the Tyr residues in -synuclein fibrillation, we modified the 3D structure of the Wild Type (WT) -synuclein and obtained the three tyrosine mutants: (Y39A; Y133A; Y(125,133,136)A)and carried out the dimerization of the Tyr mutants and WT by Potential of Mean Force (PMF) Study (Kirkwood, 1935).

From our PMF study, we observed that in the case of the dimerization of Y133A, there are less inter-molecular interactions and surface area contact between the monomeric units in comparison to the other mutants and WT. Hence we can propose that Y133A has the ability to delay the early on set of -synuclein fibrillation process. On the other hand we observed Y39A to easily form dimer and drive the monomeric units to undergo fibrillation process at a faster rate.

METHODOLOGY

A. Preparation of initial monomer structures

The initial micelle bound 3D structure of the WT (1XQ8) of -synuclein used for protein-protein interaction and Potential of Mean Force study was obtained from RCSB Protein Data Bank (Berman *et al.*, 2000). The 3D structure of Tyr mutants of -synuclein (Tyr 39 Ala, Tyr 133 Ala and Tyr (125,133,136) Ala) were obtained from the WT structure by replacing the Tyr residues with Ala at the respective positions (Fig. 1) using Swiss-Pdb viewer software (Guex *et al.*, 1997).
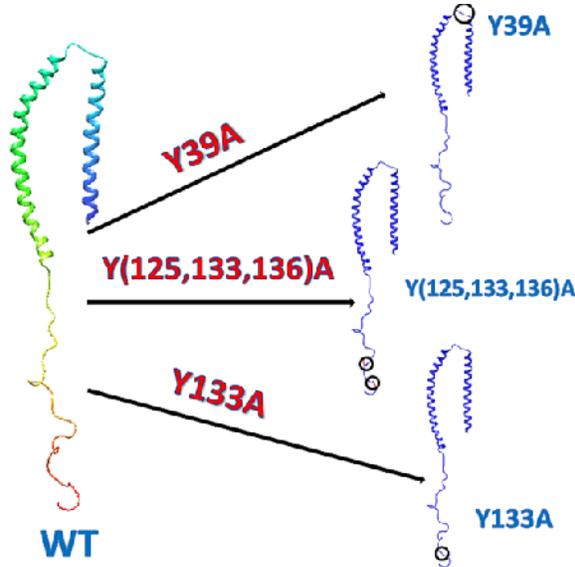

Fig. 1. Schematic representation of 3D structure of the Wild Type (WT) and Tyrosine mutants (Y39A, Y133A, Y(125,133,136)A) of -synuclein. The 3D structure of Tyrosine mutants were obtained by modifying the experimentally determined NMR structure of -synuclein (WT) using Swiss-PDB Viewer.

B. Preparation of dimer structures and Protein-Protein Interaction Study

The interaction studies of the Tyr mutants and the WT were studied using the PatchDock (Duhovny *et al.*, 2002) FireDock(Andrusier *et al.*, 2007) and PDBSum server (Laskowski, 2001). The PatchDock protein-docking server which is based on the geometry docking algorithm (Zhang *et al.*, 1997) and complementarity principles was used to dimerize the equilibrated built-in monomeric units of the Tyr mutants and WT that were obtained from Molecular Dynamics simulation and thereby analyses the top scores based on Atomic Contact Energy (ACE). PatchDock finds the optimum candidate solutions and uses the RMSD (Root Mean Square Deviation) clustering to remove redundant solutions. Based on the geometric fit as well as atomic desolvation energy (Zhang *et al.*, 1997), each solution was given a particular score. Here we have used the RMSD value to be 4 Å as default value for clustering solutions. The structures obtained from PatchDock were refined using FireDock (Andrusier *et al.*, 2007) server which is based on the Global energy algorithm. FireDock targets the flexibility problem and solutions scoring formed by fast rigid-body docking algorithms. From a total of 1000 potential docking candidate solutions, it refines according to an energy function by spending about 3.5 seconds per candidate solution. To check the protein-protein interaction, the largest ACE conformer obtained from PatchDock was submitted onto PDBSum server (Laskowski, 2001). The best recognized complex model obtained from PatchDock server was then evaluated for interface residues using PDBSum. The interface residues of a protein are defined as those residues whose contact distances from the interacting protein partner are less than 6 Å.

C. Potential of Mean Force(PMF)Study

The conformer with the largest ACE value and least global energy obtained from the PatchDock online docking server, for the three variants and WT (Fig. 2) were subjected to energy minimization, heating dynamics, density, and equilibration dynamics with the constant restraint and then proceeded for PMF study. We calculated the PMF using the Umbrella Sampling simulations (Torrie *et al.*, 1974) with the weighted histogram analysis method (WHAM)(Kumar *et al.*, 1992). For the PMF analysis, the distances between the two monomeric units of the corresponding Tyr mutants and WT were calculated as a function of inter-chain distance with Molecular Dynamics (MD) Simulation. Umbrella samples were calculated by increasing and decreasing the centre of mass distance between the two inter-monomeric units of the Tyr mutants and WT. Here, several small windows are distributed along a predefined reaction path based on MD simulation which depends on the exploration of phase space. To confine the molecular system around the selected regions of phase space, biasing potentials are added to the Hamiltonian.

The so called biasing potential is the harmonic potential (Torrie *et al.*, 1974) that keeps the system bound to the specified value in the reaction path which is done for a number of windows. For each window, the biased probability distribution (*histogram*) for the equilibrated system is obtained. As a result, the optimal free energy constant for combined simulations is determined using Weighted Histogram Analysis Method (WHAM) (Kumar *et al.*, 1992). In umbrella sampling method, the restart file of the previous step was used as the input file for the configuration in both the increasing and decreasing cases. After an increment of 1 , windows were obtained. For each window of 1 ns, NVT run was performed and for the next window the resulting equilibrated structure was used as the starting co-ordinate. Finally production run in NPT was carried out to collect the trajectories for generating the data. A harmonic potential with a spring constant of 2 kcal/mol/Å^2 was applied.

The snapshots of the three Tyr mutants(Y39A,Y133A,Y(125,133,136)A) and WT of -synuclein at different inter-monomeric distances during the course of PMF study can be seen in Fig. 3. The starting distance between the four inter-monomeric units of Tyr mutants and WT and total duration for umbrella sampling can be seen from the Table 1.
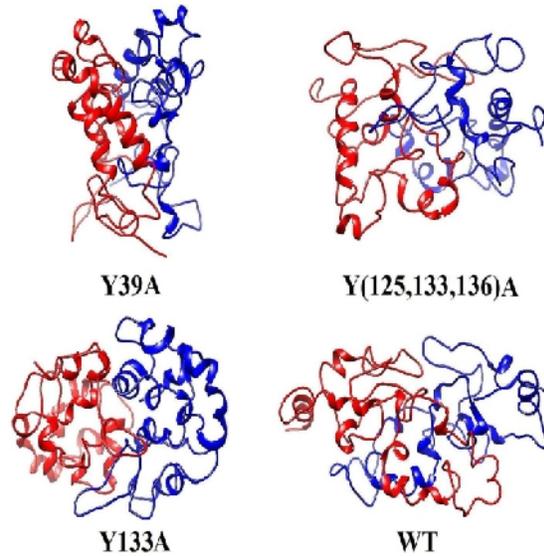

Fig. 2. The best conformers of Tyr mutants (Y39A, Y133A, Y (125,133,136) A) and WT based on Atomic Contact Energy (ACE) and global energy obtained from PatchDock online server.
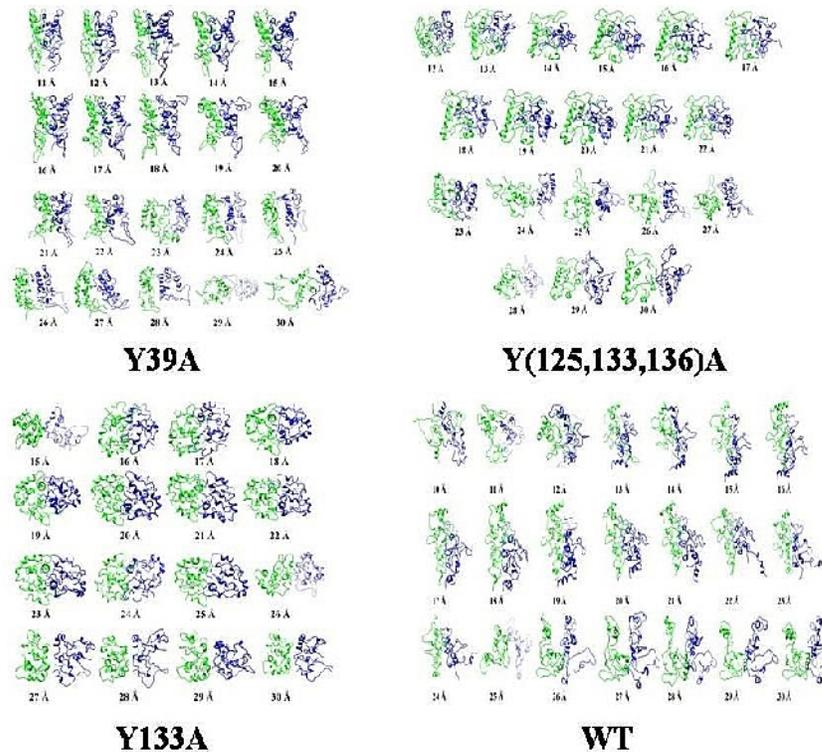

Fig. 3. Snapshot of the dimers of three Tyr (Y39A, Y133A, Y(125,133,136)A) mutants and the WT as a function of inter-monomeric distances.

Table 1: Initial and final inter-chain distance between the monomeric units of the Tyr mutants and WT - synuclein conformers with the respective global minima.

Dimer	Starting distance between COM monomer1- COM monomer2 (Å)	Distance sampled (Å)	Duration (ns) for umbrella sampling; each window size being 1 ns.	Global Minima at (Å)
Y39A	15	11 to 30	19	14.443
Y133A	20	15 to 30	15	22.1646
Y(125,133,136)A	18	12 to 30	18	18.51
WT	18	9 to 30	21	18.210

RESULTS AND DISCUSSION

A. Protein-Protein Interaction study

From the PatchDock web server, we have taken conformer of the dimers of Tyr mutants and WT based on the global free energy and ACE value. The schematic representation of the dimers of Tyr mutants and WT that we considered for inter-monomeric interaction study were shown in Fig. 2. The details regarding the geometrical shape complementarity score, interface area and ACE for the conformer of the dimers of Tyr mutants and WT were summarized in Table 2. The interface area and possible interacting residues

across the interface of the dimers were predicted using PDBSum server. The interface plot statistics (the total number of interface residues, interface area, number of salt bridges and total number of non-bonded contacts)for the dimers of Y39A, Y133A, Y(125,133,136)A and WT were summarized in Table 3. From Table 3, we observe in the case of Y39A dimer, the number of non-bonded contacts, interface residues and interface area to be higher than the other Tyr mutants and WT. This indicates that Y39A readily forms a stable dimer than the other Tyr mutants and WT. The individual residue-residue interactions across the interfaces along with involved residues in the dimers of Tyr mutants and WT were shown in Fig. 4.

Table 2: PatchDock results for the Tyr mutants and WT showing the geometric shape complementarity score, interface area and atomic contact energy.

Dimer	Geometric shape complementarity Score	Interface Area (Å)^2	Atomic Contact Energy (kcal/mol)
Y39A	15112	2906.60	-97.00
Y133A	15416	2374.90	156.12
Y(125,133,136)A	14996	2421.60	-475.42
WT	15918	1981.30	30.11

Table 3: Interface plot statistics of the homo dimer Y39A, Y133A, Y(125,133,136)A and WT showing the total number of interface residues, interface area, number of salt bridge and total non-bonded contacts.

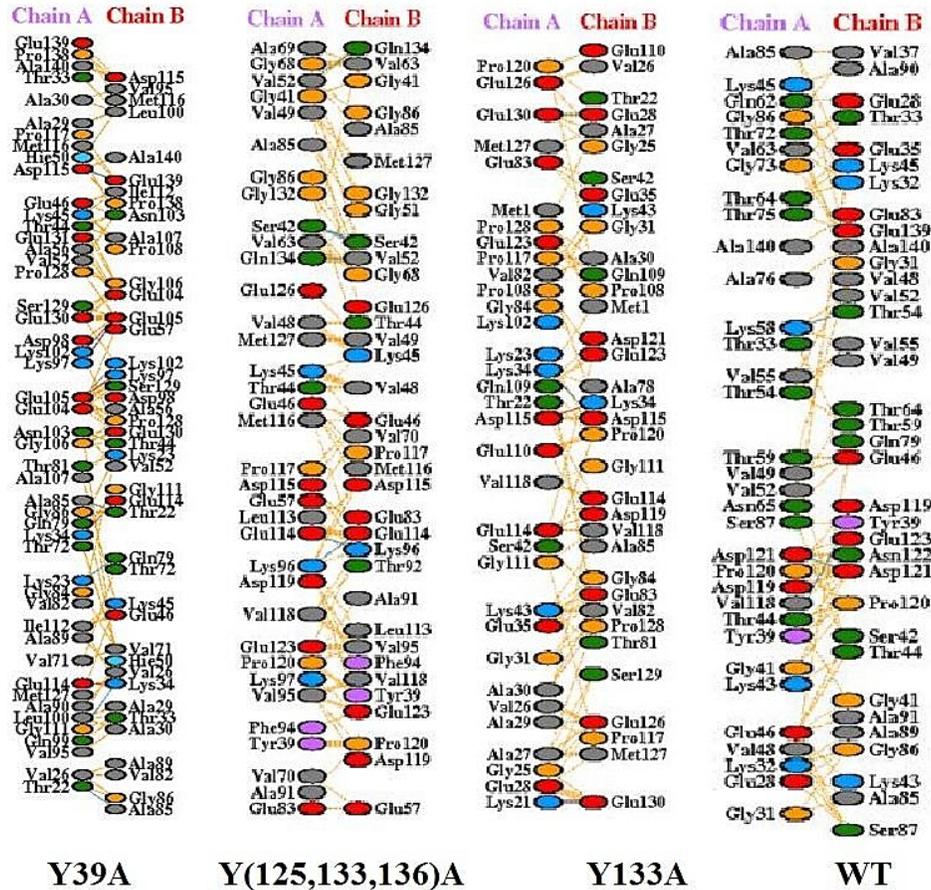| Dimer	Chain	No of interface residues	Interface area (Å^2)	No of salt bridges	No of disulphide bonds	No of hydrogen bonds	No of Non-bonded contacts
Y39A	A	48	2130	5	-	7	619
	B	43	2186				
Y133A	A	33	1648	3	-	3	498
	B	35	1701				
Y(125,133,136)A	A	35	1783	-	-	6	385
	B	35	1788				
WT	A	33	1526	-	-	3	402
	B	35	1557				

Fig. 4. Intermolecular interactions in the dimers of Tyr mutants (Y39A, Y133A, Y(125,133,136)A) and WT -Synuclein. Orange line denotes non-bonded contacts, red line denotes slat-bridges and blue line denote hydrogen bond.

B. Potential of Mean Force Study

Molecular Dynamics Simulations along with Umbrella sampling were used to study the dissociation of the dimers of Tyr mutants and WT in terms of the free energy profiles. The Potential of Mean Force (PMF) and inter-molecular potential energy were computed in the dimers in two different direction of separation as functions of distance between centre of masses of the two monomeric units. Fig. 5 illustrates the PMF profiles of the dimers of Tyr mutants and WT as a function of inter-monomeric distance in angstroms (Å). The equilibrated snapshots from the MD trajectories were chosen as the initial conformations for the umbrella sampling simulations for this study. 1 ns Umbrella sampling simulation was performed for each window to assure the convergence of sampling in the simulations. The convergence of the PMFs for each system was validated by performing Umbrella Sampling simulations.
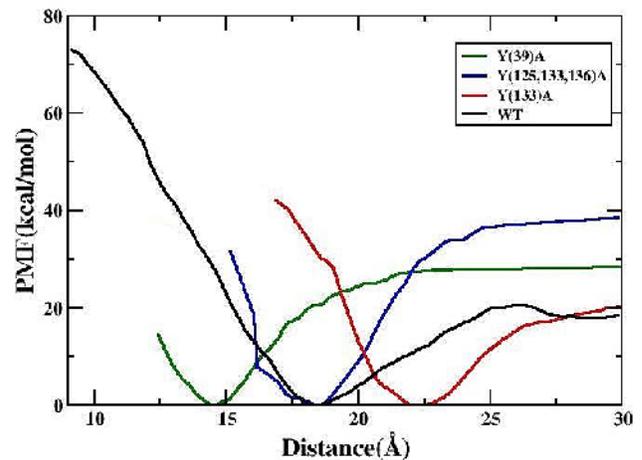

Fig. 5. PMF plot for the mutants (Y39A, Y133A, Y(125,133,136)A) and WT of -synuclein showing the varying optimal distance and the attractive and repulsive forces that are holding the dimers.

From the PMF plot (Fig. 5), the separation between the two monomeric units along the centre of mass (COM) can be observed for constant temperature of 300 K. It is clearly seen from the plot that when the distance between the centre of masses of two monomeric units is between than 20-30 the PMF value decreases for the Tyr mutants and WT. As the attractive forces comes to a minimal point, the global minima for the mutants and WT is achieved wherein the optimal values are noted. The PMF profile indicates that a presence of a minimum of separation of monomeric units in dimers and the energy barrier to dissociation for Tyr mutants and WT to be: Y39A-Y39A (14.2 Å, 28 kcal/mol); Y (125,133,136) A-Y(125,133,136)A (18.5 Å, 38 kcal/mol); WT-WT (18.2 Å, 19 kcal/mol); Y133A-Y133A (22.16 Å, 17 kcal/mol). In the case of dimerization of Y39A, we observed the minimum of separation of monomeric units to be lesser when compared to other Tyr mutants and WT of -synuclein. Whereas for mutant, Y133A the distance between the monomeric units are far apart from one another and hence the attractive forces is the least when compared to others. From these observations, we can infer Y39A has the ability to initiate the aggregation propensity as it can easily form dimer which further form toxic intermediates and influence the fibrillation propensity as studied earlier (Ulrih *et al.*, 2008). Hence numerous drugs can be discovered which can be a useful for targeting the -synuclein protein and its variants.

C. Solvent Accessible Surface Area (SASA) for the NAC (non-amyloid component) region

To check finer details about the mobility of the flexible regions present in the dimer of WT and Tyr mutants of -synuclein, we calculated the SASA exclusively for the NAC region. We analyzed the accessible surface area of NAC region in the monomeric units of the dimers of Tyr mutants and WT. For this analysis, we have used the Molecular Dynamics trajectory of the lowest energy conformer of the dimers of Tyr mutants and WT (Fig. 6). From Fig. 6, we observed accessible surface area of non-amyloid -component region (which is important for aggregation) to be larger in the case of dimer of Y39A than the other Tyr mutants and WT of -synuclein. So we infer that Y39A mutation in -synuclein accelerates the aggregation propensity than the WT and other Tyr mutants. While in Y133A and Y(125,133,136)A mutants we noticed the accessible surface area in NAC region to be lower.
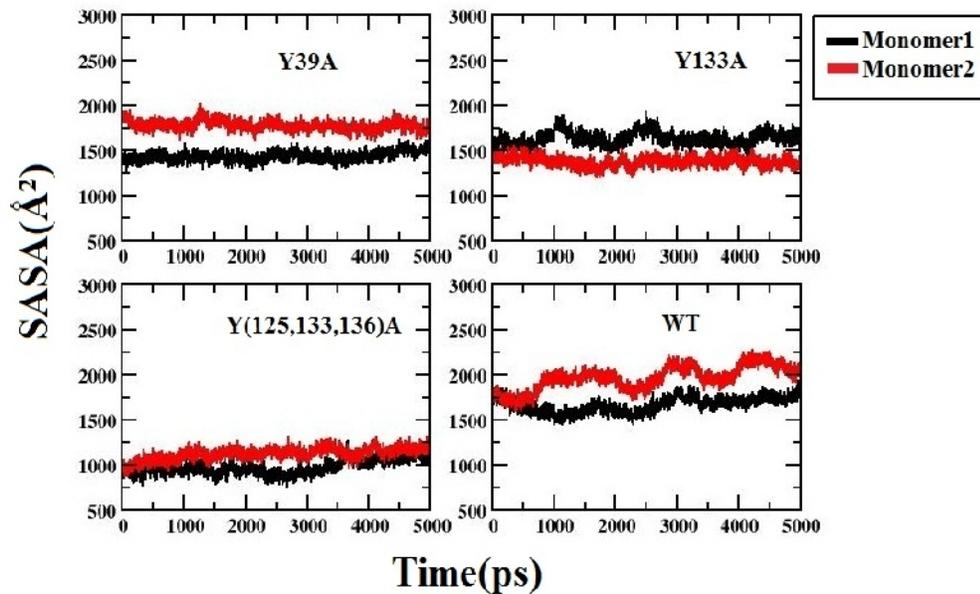

Fig. 6. Solvent Accessible Surface Area analysis (SASA) for the Tyr mutants (Y39A, Y133A, Y(125,133,136) A) and WT of -synuclein for the NAC (non-amyloid component) region.

CONCLUSIONS

The involvement of tyrosine residues of -synuclein in the inter-molecular interactions during the dimerization process was studied. From our study, we can see among the tyrosine mutants, Y133A has the capacity to delay the fibrillation propensity of -synuclein as it shows a substantially different conformation than the other tyrosine mutants. Among the three mutants (Y133A, Y39A, Y(125,133,136)A) and the WT, we found the inter-molecular interactions to be stronger in case of Y39A and weaker in Y133A.

These findings suggest that the aggregation propensity of -synuclein protein will be higher when it has Y39A mutation and lower when it has Y133A mutation. This is in agreement with the work that has been reported earlier (Ulrih *et al.*, 2008). Therefore we see Y39A mutation to accelerate the -synuclein aggregation while Y133A slow down the aggregation. So the methods targeting tyrosine residue at position 133 may be focused to reduce the aggregation propensity of -synuclein.

ACKNOWLEDGEMENTS

REFERENCES

Bendor, J. T., Logan, T. P. & Edwards, R.H. (2013). The function of -synuclein. *Neuron.***79**, 1044–1066. http://dx.doi.org/10.1016/j.neuron.2013.09.004.

Berman, H.M., Westbrook, J., Feng, Z., Gilliland, G., Bhat, T.N., Weissig, H., Shindyalov, I.N. & Bourne, P.E. (2000). The protein data bank. *Nucleic Acids Research.* 28235-242.

Bertoncini, C. W., Jung, Y. S., Fernandez, C. O., Hoyer, W., Griesinger, C., Jovin, T. M. & Zweckstetter, M. (2005). Release of long-range tertiary interactions potentiates aggregation of natively unstructured alpha-synuclein. *Proc. Natl. Acad. Sci.* **102**, 1430–435.http://dx.doi.org/10.1073/pnas.0407146102.

Bisaglia, M., Mammi, S., & Bubacco, L. (2009). Structural insights on physiological functions and pathological effects of alpha-synuclein. *FASEBJ.* **23**, 329–340. doi: 10.1096/fj.08-119784.

Breydo, L.J., Wu, W. & Uversky, V. N. (2012). -synuclein misfolding and Parkinson's disease. *BBA-Mol. Basis Dis.***1822**, 261-285.

Cremades, N., Cohen, S. L., Deas, E., Abramov, A. Y., Chen, A.Y., Orte, A., Sandal, M., Clarke, R.W., Dunne, P., Aprile, F.A., Bertoncini, C.W., Wood, N.W., Knowles, T.P.J., Dobson, C.M. & Klenerman, D. (2012). Direct observation of the interconversion of normal and toxic forms of -synuclein. *Cell.* **149**, 1048-1059. http://dx.doi.org/10.1016/j.cell.2012.03.037.

Duhovny, D., Nussinov, R., & Wolfson, H.J. (2002). Efficient unbound docking of rigid molecules. Italy: Springer.

Dusa, A., Kaylor, J., Edridge, S., Bodner, N., Hong, D. P. & Fink, A. L. (2006). Characterization of oligomers during alpha-synuclein aggregation using intrinsic tryptophan fluorescence. *Biochemistry.* **45**, 2752-2760.

http://dx.doi.org/10.1021/bi051426z.

Fauvet, B., Fares, M.B., Samuel, F., Dikiy, I., Tandon, A., Eliezer, D. & Lashuel, H.A. (2012). Characterization of semi-synthetic and naturally N -acetylated -synuclein in vitro and in intact cells: implications for aggregation and cellular properties of -synuclein. *J. Biol. Chem.* **287**, 28243-28262.

Fink, A.L. (2006). The aggregation and fibrillation of alpha-synuclein. *Accounts Chem. Res.* **39**, 628-634.http://dx.doi.org/10.1021/ar050073t.

Gazit, E. (2002). A possible role for pi-stacking in the self-assembly of amyloid fibrils. FASEB J.16, 77-83.http://dx.doi.org/10.1096/fj.01-0442hyp

Giasson, B. I., Murray, I. V. J., Trojanowski, J.Q. & Lee, V.M.Y.(2001). A hydrophobic stretch of 12 amino acid residues in the middle of alpha-synuclein is essential for filament assembly. *J. Biol. Chem.* **276**, 2380-2386.http://dx.doi.org/10.1074/jbc.M008919200.

Guex, N. & Peitsch, M.C. (1997). SWISS-MODEL and the Swiss-pdb viewer: an environment for comparative protein modeling. Electrophoresis. 182714-2723.

Iwai, A., Masliah, E., Yoshimoto, M., Ge, N., Flanagan, L., de Silva, H.A., Kittel, A., & Saitoh, T. (1995). The precursor protein of non-A b component of Alzheimer's disease amyloid is a presynaptic protein of the central nervous system. *Neuron.* **14**: 467-475.

Izawa, Y., Tateno, H., Kameda, H., Hirakawa, K., Hato, K., Yagi, H., Hongo, K., Mizobata, T. & Kawata, Y. (2012). Role of C-terminal negative charges and tyrosine residues in fibril formation of ?-synuclein. Brain Behav.2, 595-605.http://dx.doi.org/10.1002/brb3.86.

Kirkwood, J.G. (1935). Statistical mechanics of fluid mixtures. *Journal of Chemical Physics.* **3**, 300-313.

Kumar, S., Bouzida, D., Swendsen, R.H., Kollman, P.A. & Rosenberg, J.M. (1992). The Weighted Histogram Analysis Method for Free-Energy Calculations on Biomolecules. I. The Method, *Journal of Computational Chemistry*. Vol. **13**, No. 8, 1011-1021.

Lamberto, G. R., Binolfi, A., Orcellet, M. L., Bertoncini, C. W., Zweckstetter, M., Griesinger, C. & Fernandez, C. O. (2009). Structural and mechanistic basis behind the inhibitory interaction of PcTS on alpha-synuclein amyloid fibril formation. Proc. Natl. Acad. Sci. USA.106, 21057-21062. http://dx.doi.org/10.1073/pnas.0902603106.

Laskowski, R.A. (2001). PD Bsum: summaries and analyses of PDB structures. *Nucleic Acids Research.* **29**(1), 221-222.

Pirc, K., Ulrih, N. P. & Rana, A.Q. (2011).(Ed.): Etiology and physiology of Parkinson's disease, Intech, Rijeka, Croatia, pp. 87-110.

Serpell, L.C., Berriman, J., Jakes, R., Goedert, M., & Crowther, R.A. (2000). Fiber diffraction of synthetic -synuclein filaments shows amyloid-like cross-b conformation. *Proc. Natl. Acad. Sci.* **97**: 4897-4902.

Torrie, G. M. & Valleau, (1974). Modeling Condensed Phase Reaction Dynamics J. P. *Chem. Phys. Lett.* **28**, 578-581.

Ulrih, N. P., Barry, C. H. & Fink, A. L. (2008). Impact of Tyr to Ala mutations on alpha-synuclein fibrillation and structural properties. *BBA-Mol. Basis Dis.* **1782**, 581-585.

Uversky, V.N., Li, J. & Fink, A.L. (2001). Evidence for a partially folded intermediate in -synuclein fibril formation. *J. Biol. Chem.* **276**, 10737-10744.

Uversky, V.N., Oldfield, C.J., Midic, U., Xie, H., Xue, B., Vucetic, S., Iakoucheva, L.M., Obradovic, Z. & Dunker, A.K. (2009). Unfoldomics of human diseases: linking protein intrinsic disorder with diseases. *BMC Genomics*. **10**(Suppl 1):S7DOI: 10.1186/1471-2164-10-S1-S7.

Weinreb, P.H., Zhen, W., Poon, A.W., Conway, K.A., & Lansbury Jr., P.T. (1996). NACP, a protein implicated in Alzheimer's disease and learning, is natively unfolded. *Biochemistry*. **35**: 13709-13715.

Yamin, G., Uversky, V.N. & Fink, A.L. (2003). Nitration inhibits fibrillation of human alpha-synuclein in vitro by formation of soluble oligomers. *FEBS Lett.* **542**,147-152. http://dx.doi.org/10.1016/S0014-5793(03)00367-3.

Zhang, C., Vasmatzis, G., Cornette, J.L. & DeLisi, C. (1997). Determination of atomic desolvation energies from the structures of crystallized proteins. *Journal of Molecular Biology*. **267**(3), 707-726.